Journal of Autoimmunity 138 (2023) 103053

Contents lists available at ScienceDirect

Journal of Autoimmunity

journal homepage: www.elsevier.com/locate/jautimm

HNF4α, SP1 and c-myc are master regulators of CNS autoimmunity

Emanuela Colombo [a,1], Marco Di Dario [a,1,2], Ramesh Menon [a], Maria Maddalena Valente [a], Claudia Bassani [a], Nicole Sarno [a], Davide Mazza [b], Federico Montini [a], Lucia Moiola [a], Giancarlo Comi [a], Vittorio Martinelli [a], Cinthia Farina [a,*]

[a] Institute of Experimental Neurology (INSpe), Division of Neuroscience, IRCCS Scientific Institute San Raffaele, Milan, Italy
[b] Experimental Imaging Center, IRCCS Scientific Institute San Raffaele, Milan, Italy

ARTICLE INFO

Handling Editor: M.E. Gershwin

Keywords:
C -myc
Cigarette smoke
CNS autoimmunity
EAE
HNF4α
Immune activation
Multiple sclerosis
Master regulator
SP1
Vitamin D

ABSTRACT

Hepatocyte nuclear factor 4 α (HNF4α), a transcription factor (TF) essential for embryonic development, has been recently shown to regulate the expression of inflammatory genes. To characterize HNF4a function in immunity, we measured the effect of HNF4α antagonists on immune cell responses in vitro and in vivo. HNF4α blockade reduced immune activation in vitro and disease severity in the experimental model of multiple sclerosis (MS). Network biology studies of human immune transcriptomes unraveled HNF4α together with SP1 and c-myc as master TF regulating differential expression at all MS stages. TF expression was boosted by immune cell activation, regulated by environmental MS risk factors and higher in MS immune cells compared to controls. Administration of compounds targeting TF expression or function demonstrated non-synergic, interdependent transcriptional control of CNS autoimmunity in vitro and in vivo. Collectively, we identified a coregulatory transcriptional network sustaining neuroinflammation and representing an attractive therapeutic target for MS and other inflammatory disorders.

1. Introduction

HNF4α is a member of the nuclear receptor superfamily of ligand-dependent transcription factors (TFs) [1]. Necessary for proper development and highly expressed in the liver, kidney, small intestine, colon and pancreatic cells, it regulates the expression of genes involved in processes such as lipid, glucose and protein metabolism, hematopoiesis and blood coagulation [2]. Described for a long time as an orphan receptor, it binds to fatty acyl-CoA but not free fatty acids or CoA, and, while saturated fatty acyl-CoA with chains of 14 and 16 carbon atoms promote HNF4α transcriptional activity, ω-3 polyunsaturated fatty acyl-CoA and saturated long-chain fatty acids inhibit its function [3,4]. Interestingly, HNF4α controls sexually dimorphic gene expression in the liver [5], and has been identified as a candidate epigenetic interactor of genes differentially expressed in immune cells of male and female patients affected by multiple sclerosis (MS) [6]. MS is a chronic disorder of the central nervous system (CNS), characterized by demyelination, neurodegeneration, immune cell dysregulation in the periphery and infiltration in the nervous tissue [7–10]. As HNF4α may induce the expression of inflammatory genes [11] and abundance of agonistic HNF4α ligands and deficiency in antagonistic fatty acids are reported in MS plasma [12], here we hypothesized a direct role for HNF4α in immune function, MS and its experimental model, the experimental autoimmune encephalomyelitis (EAE). Moreover, we postulated and verified the existence of more complex TF networks implied in MS, regulated by known MS risk factors and controlling immunity in vitro and in vivo.

Abbreviations: aVitD3, 1α,25-dihydroxyvitamin D3; CIS, clinically isolated syndromes; ConA, Concanavalin A; CS, cigarette smoke; DEG, differentially expressed gene; EAE, experimental autoimmune encephalomyelitis; LPS, lipopolysaccharide; MS, multiple sclerosis; PBMC, Peripheral blood mononuclear cell; PP-MS, primary progressive MS; RR-MS, relapsing-remitting MS; SP-MS, secondary progressive MS; TF, transcription factor; TFNA, transcription factor network analysis.

* Corresponding author. Institute of Experimental Neurology (INSpe) and Division of Neuroscience, San Raffaele Scientific Institute, Via Olgettina, 58, 20132, Milan, Italy.
E-mail address: farina.cinthia@hsr.it (C. Farina).

[1] These authors contributed equally.
[2] Present address: Department of Diagnostic Services, San Paolo Hospital, ASST Santi Paolo e Carlo, Milan, Italy

https://doi.org/10.1016/j.jaut.2023.103053
Received 23 September 2022; Received in revised form 6 March 2023; Accepted 3 May 2023
Available online 24 May 2023

2. Materials and methods

2.1. Animals and experimental autoimmune encephalomyelitis (EAE)

All procedures involving animals were authorized by the Institutional Animal Care and Use committee of the San Raffaele Scientific Institute and the Italian General Direction for Animal Health at the Ministry of Health. Wild type C57BL/6 N female mice were purchased from Harlan laboratories and housed in the institutional facility providing constant temperature (22 ± 1 °C), humidity (50%) and 12 h light/dark cycle. They had ad libitum access to food and water. EAE was induced in 8-week-old wild type C57BL/6 N female mice by subcutaneous injection of 200 μg MOG_{35-55} peptide emulsified in complete Freund's adjuvant (BD Biosciences) containing 5 mg/ml Mycobacterium tuberculosis (BD Biosciences). Bordetella pertussis toxin (List-Quadratech) was administered by intra-peritoneal (i.p.) injection at the day of immunization (400 ng/mouse) and 2 days later (200 ng/mouse). Animals were monitored daily and scored as follows: 0 = no disease; 1 = flaccid tail; 2 = gait disturbance; 3 = complete hind limb paralysis; 4 = tetraparesis and 5 = death as previously described [6,13]. Three mg/kg/day BIM5078 (HNF4α inhibitor, Cayman Chemicals), BI6015 (HNF4α inhibitor, Merck Millipore), WP631-dimethansulfonate (SP1 inhibitor, Zageno) and OTX015 (c-myc inhibitor, Selleckchem) were orally administered to C57BL/6 N immunized mice at day 7 post-immunization or three days after disease onset. Eventually, drug treatments were discontinued after day 31 post immunization. Control mice received administration of vehicle (0,12% DMSO v/v in 0.9% NaCl physiologic solution). Experimenters were blind to treatment regimen of EAE mice.

2.2. Recruitment of human subjects, blood sampling and PBMC preparations

All procedures in studies involving human subjects were approved by the Ethical Committee at San Raffaele Scientific Institute and performed in accordance with the ethical standards as laid down in the 1964 Declaration of Helsinki and its later amendments or comparable ethical standards. Informed consent was obtained from all participants to the study. Blood sampling was performed between 9 and 12 a.m. MS patients enrolled in this study were classified in accordance to McDonald's criteria [14] and none of them was suffering from other inflammatory and autoimmune disorders and was under immunomodulatory or immunosuppressive therapy. Similarly, blood samples were obtained from healthy donors. Peripheral blood mononuclear cells (PBMC) were isolated from anticoagulated whole blood as previously described [6] and immediately used for in vitro assays.

2.3. PBMC stimulation

PBMC were counted by Trypan Blue exclusion (Sigma-Aldrich, Milan, Italy) and resuspended in RPMI 1640 (Thermo Fisher Scientific) supplemented with 5% fetal bovine serum (FBS), 1% glutamine and 1% penicillin/streptomycin (Euroclone). Cells were seeded in 96-well round bottom plates at the concentration of 2×10^5 cells/well. PBMC were exposed for 4 h to HNF4α inhibitors BIM5078 (Cayman Chemicals) or BI6015 (Merck Millipore), SP1 inhibitor WP631-dimethansulfonate (Zageno), c-myc inhibitor OTX015 (Selleckchem), cigarette smoke conditioned media (CS, prepared as described in Bernhard et al., 2004) and 41,6 pg/ml 1,25-Dihydroxyvitamin D3 (aVitD3) (Tocris). After this incubation, immune cell activation was triggered for 18 h (for cytofluorimetric or immunofluorescence analyses) or 3 days (for proliferation assays) with appropriate stimuli: lipopolysaccharide (LPS; 1 μg/mL) (Sigma-Aldrich) and Concanavalin A (ConA; 2,5 μg/mL) (Sigma-Aldrich) for monocyte and T lymphocyte activation, respectively.

2.4. Flow cytometry

PBMC were labeled with antibodies against CD3 (1:50, Biolegend) and CD14 (1:50, Biolegend), for T lymphocyte or monocyte discrimination, respectively. Antibodies against CD25 (1:50, Biolegend), CD150 (1:10, Biolegend) and CD69 (1:400, Biolegend) were used to evaluate immune cell activation and 7AAD (Biolegend) for cell viability. Samples were acquired at BD FACSCanto II (BD Biosciences) and analyzed by FlowJo software (Tree Star Inc). Thresholds for positive stainings were fixed on the corresponding isotype controls. In each experiment 2 to 3 technical replicates were analyzed.

2.5. RNA extraction, cDNA synthesis and qualitative PCR amplification

Total RNA from PBMC was extracted by TriReagent (Thermo Fisher Scientific), quantified at NanoDrop spectrophotometer and reverse transcribed using random primers and Superscript III reverse transcriptase (Thermo Fisher Scientific). Qualitative RT-PCR was performed using GoTaq G2 DNA polymerase (Promega) and dNTPs set (Thermo Fisher Scientific). The specific HNF4α primers were designed as follows: Exon 3–4 (Fw primer CATCAGAAGGCACCAACCTC, Rev primer GGCACTGGTTCCTCTTGTCT), Exon 3–8 (Fw primer GAGATCCATGGTGTTCAAGGA, Rev primer ATGATGGCTTTGAGGTAGGC), Exon 7–8 (Fw primer GAGATCCATGGTGTTCAAGGA, Rev primer ATGATGGCTTTGAGGTAGGC). PCR products were separated by electrophoresis in 2% agarose gel and visualized by SYBR-safe (Thermo Fisher Scientific) staining. Human liver mRNA was used as positive control and processed as described above. Negative control (amplification mix without any cDNA) was used to exclude any contamination. The reaction was performed according to the following conditions: 2 min at 95 °C; 40 cycles of 20 s at 95 °C, 20 s at 55 °C, 30 s at 72 °C, and a final extension period of 10 min at 72 °C in Mini Thermal Cycler (Bio-Rad).

2.6. Microarray experiments and differential gene expression analysis

Total RNA from untreated and BI6015-treated PBMC was used for gene expression profiling with Illumina HT-12-v4 arrays (Illumina). RNA quality was checked at Bionalyzer 2100 (Agilent Technologies). Reverse transcription and biotinylated cRNA synthesis were performed using the Illumina TotalPrep RNA Amplification Kit (Thermo Fisher Scientific), according to the manufacturer's protocol. Array hybridization, washing, staining and scanning in the Beadstation 500 (Illumina) were performed according to standard Illumina protocols. The summary probe profile was exported to R/Bioconductor platform [15] to perform pre-processing (filtering for detection pvalue$<$0.05 and intensity $>$100 in at least one experimental group) and differential expression analysis (eBayes p value $<$ 0.01).

PBMC transcriptomes relative to 186 healthy, CIS and MS subjects (see Table S2 for demoraphic and clinical features) were generated with HumanRef-8 v2 arrays (ArrayExpressID E-MTAB-11415). The raw intensities were background subtracted using nec function in LIMMA package [16,17] which performs background correction using negative control probes. The data were normalized using cubicspline method and the probes were filtered if detected (p value $<$ 0.01) in at least 20% of samples. Finally, the filtered 11,184 probes were log2 transformed and were subjected to batch correction using ComBat package [18], in order to nullify the bias due to different hybridizations time points. Towards the identification of differentially expressed genes, the samples were divided into screening and validation groups (ratio ~ 50:50, Table S2). We used three parallel statistical methods to identify the differentially expressed genes. A differentially expressed gene was the one that passed any of the two tests in the screening group and at least one test in the validation group. The statistical tests were Welch *t*-test (p-value $<$0.05), Significant Analysis of Microarrays (fdr $<$0.2) and LIMMA (p-value $<$0.05). Genes deregulated by the healthy aging were identified by

measuring the Spearman's rank correlation between the age and expression level in the healthy group. The correlation coefficient threshold was set to ±0.5 (p-value <0.01).

2.7. Transcription factor network analysis (TFNA)

TFNA was performed using Metacore (Thomson Reuters). This tool considers the downstream targets of transcriptional regulation by the TF and also all possible types of interactions between a DEG and the TF described in the literature. Thus, TFNA derives interactomes for each TF interacting with DEG and calculates the statistical significance (hypergeometric test). Of note, p-values are normalized for the generated networks, meaning that the statistical test considers all the interacting nodes among the given user input (DEG list). Metacore tool provides the z-score as secondary indication of statistical significance.

2.8. Immunofluorescence and confocal microscopy

PBMC cultures were fixed with 4% paraformaldehyde for 10 min at RT, permeabilized for 1 h at RT (2% BSA, 2% FBS, 0,1% Triton X-100 buffer) and then incubated with primary antibodies diluted in 10% FBS-0,1% Triton X-100 solution and directed against HNF4α (1:1000, Abcam), SP1 (1:50, Santa Cruz Biotechnology), c-myc (1:200, Abcam), CD3 (1:600, Biolegend), CD4 (1:50, Biolegend), CD8 (1:50, Biolegend) and CD14 (1:600, Biolegend) or isotype controls. After overnight incubation at 4 °C, cells were washed two times with PBS and then incubated 1 h at room temperature with the following secondary antibodies: Alexa Fluor 488 or 594 anti-mouse Ig (1:1000, Thermo Fisher Scientific) and Alexa Fluor 488 or 647 anti-rabbit Ig (1:1000, Thermo Fisher Scientific). Nuclei were labeled with DAPI (1:10000, Sigma-Aldrich). Cells were fixed on slides after cytospin centrifugation (3' at 900 rpm, medium speed, Thermo Shandon). To quantify nuclear HNF4α, SP1 and c-myc, DAPI images were converted to 8-bit, and regions of interest (ROIs) were generated to select (DAPI positive) nuclei. Then ROIs were applied to the corresponding HNF4α/SP1/c-myc images and fluorescence thresholds were fixed on the unstimulated condition. The area of positive nuclear signal was quantified and expressed as percentage of total nuclear area. For each condition 2 to 3 technical replicates were analyzed. Images were captured at Leica TCS SP5 confocal laser-scanning microscope equipped with 40 × and 63 × oil objectives. Acquisition settings were set on negative controls and single stacks were acquired by LASAF and LASX softwares. ImageJ software was used for image analysis by blinded investigators.

2.9. Super-resolution microscopy

For super-resolution images PBMC were stained as mentioned above. Direct stochastic optical reconstruction microscopy (dStorm) was used to determine localization imaging [19]. dStorm was performed on a Leica SR GSD-3D (Leica Microsystems Srl) super-resolution microscope equipped with a 150 × 1.45NA objective, an Andor iXon Ultra-897 EM-CCD sensor and three solid state lasers. The samples were mounted on the stage and the medium was substituted prior to acquisition with the TN buffer (560 μg/ml glucose oxidase, 400 μg/ml catalase and 100 mM cysteamine HCl) supplemented with 10% glucose (w/v) pH 8.0, to induce blinking of the fluorophores. Alexa 568 and Alexa 647 were imaged sequentially (starting from the far-red channel). 40.000 images were collected for each channel with 8 ms exposure times and an increasing ramp of 405 nm laser intensity with powers between 0 and 0.8 mW was used to reactivate the molecules in long-lived dark states. Localization events with less than 20 photons/pixel for the Alexa 647 dye and 30 photons/pixels for the Alexa 568 dye were discarded. The super-resolution images were reconstructed as 2D histograms for visualization purposes (pixel size: 20 nm).

2.10. ELISA

Human TNF-α, IFN-γ and IL-17 levels were measured in PBMC supernatants by ELISA MAX™ Standard Set (Biolegend) according to the manufacturer's protocol. Colorimetric read-out was analyzed by Epoch Micro-Volume Spectrophotometer System (Biotek). Experiments were performed in duplicates.

2.11. T cell proliferation assays

Spleen and lymph node cells were isolated from naïve or EAE mice, seeded in 96-well round bottom plates in complete RPMI medium and preincubated in vitro with vehicle, BIM5078, CS or aVitD3. Alternatively, spleen and lymph nodes cells were derived from EAE mice treated with vehicle or TF inhibitors. Cells then were stimulated with increasing concentrations of MOG_{35-55} peptide or ConA (5 μg/ml). T cell proliferation was also investigated in PBMC eventually treated with BIM5078 and stimulated with ConA. After 72 h cultures were pulsed for 18 h with 0.5 mCi/well of [3H] thymidine and harvested. Thymidine incorporation was measured from quadruplicate cultures per condition on a β-counter (PerkinElmer) and data were reported as proliferation index [cpm + antigen/cpm media].

2.12. Quantification and statistical analysis

Quantification details are provided along the methods section and in figure legends. Details about the statistical methods, the exact number of mice, samples or performed independent experiments are reported in figure legends. Statistical analyses were performed in Excel or GraphPad Prism. Normality of data distribution was assessed by Kolmogorov-Smirnov statistics. Student *t*-test (in case of normal distribution) or non-parametric Mann-Whitney *U* Test (in case of non-normal distribution) were performed to compare means. For statistical evaluation of EAE score and proliferation assays, linear regression analysis with 95% confidence interval was used. For microarray experiments and differential gene expression analysis, statistical methods are described in the relative methods section. In figures, asterisks denote statistical significance as *p < 0.05; **p < 0.01; ***p < 0.001, ****p < 0.0001.

3. Results

3.1. HNF4α modulates immune cell function in vitro and in vivo

Molecular biology and immunofluorescence experiments demonstrated HNF4α mRNA in human peripheral blood mononuclear cells (PBMC) from healthy subjects (Fig. 1A and B) and HNF4α protein in CD4 and CD8 positive T lymphocytes (Fig. 1C left panels) and monocytes (CD14 positive cells, Fig. 1C right panel). To dissect the role of this TF in immune function, we inhibited its activity by two antagonists, BIM5078 and BI6015, that specifically bind HNF4α ligand-binding pocket and block its transcriptional activity [20]. In a first set of experiments, we evaluated human immune cell activation in the presence of the antagonists in vitro. Briefly, PBMC were exposed to non-toxic concentrations of inhibitors (Figs. S1A–B) for 4 h and then stimulated with ConA and LPS to induce T lymphocyte or monocyte activation respectively. After 18 h of stimulation, cells were recovered and immune cell activation (via CD25 and CD69 staining for T lymphocytes, and CD25 and CD150 staining for monocytes [21,22]) was analyzed by flow cytometry. BIM5078 significantly reduced the induction of activation markers on T lymphocytes (Fig. 1D and E) and monocytes in a concentration-dependent manner (Fig. 1F and G). Consistently, this action resulted in the inhibition of ConA-induced production of IFN-γ and IL-17 by T lymphocytes (Fig. S1C) and of LPS-induced TNF-α release by monocytes (Fig. S1D). Similarly, BI6015 dramatically reduced the expression of all activation markers on T lymphocytes (Fig. 1H and I) and monocytes (Fig. 1J and K). Transcriptomics analysis of PBMC

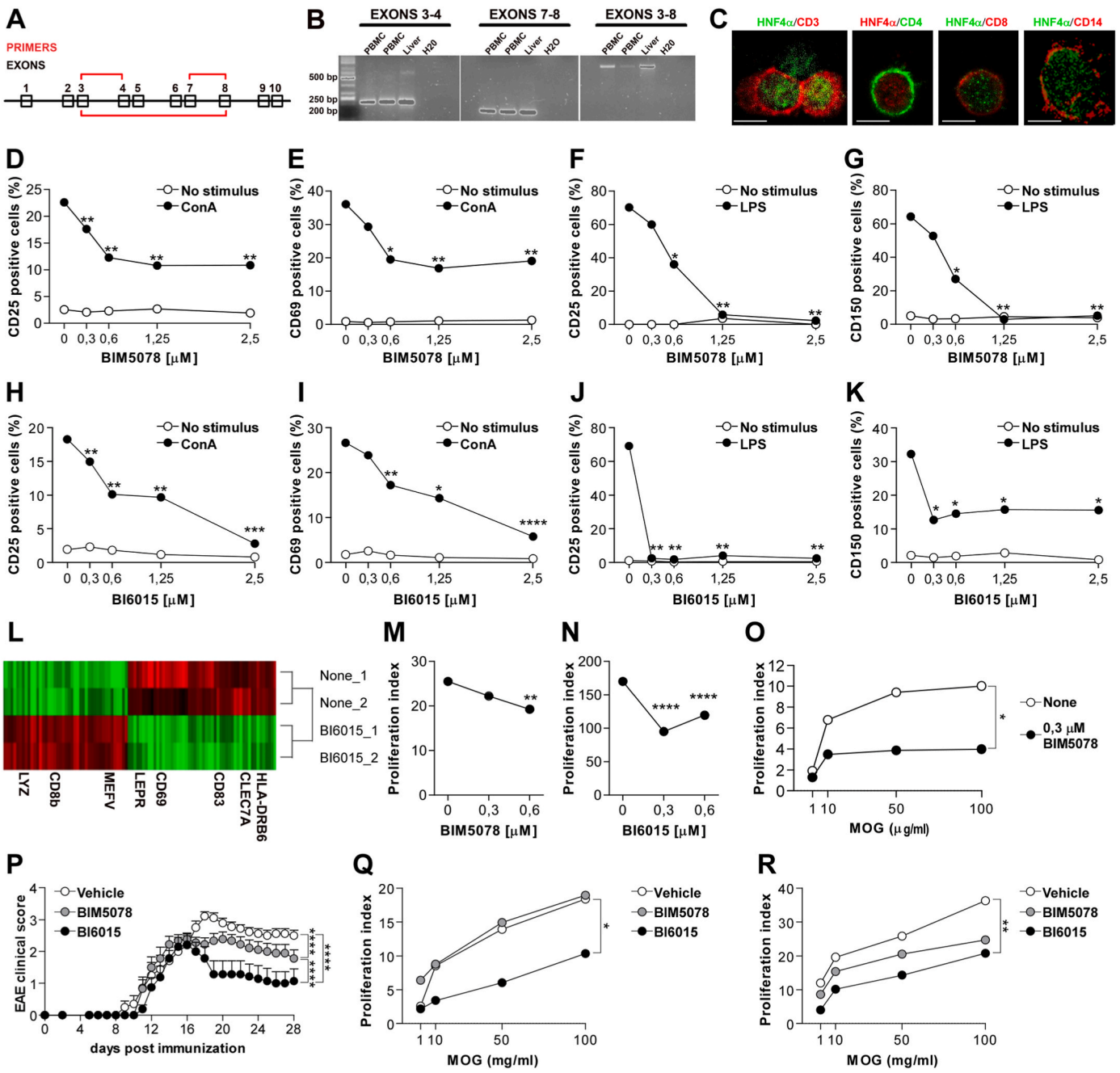

Fig. 1. HNF4α is expressed by human T cells and monocytes, where it regulates cell activation (A) Schematic representation of three different primer combinations designed to evaluate HNF4α expression by qualitative RT-PCR. (B) HNF4α transcript expression in human PBMC by RT-PCR. cDNA was extracted from PBMC of two healthy donors. cDNA from human liver was used as positive control. (C) Representative images of HNF4α protein expression in CD3, CD4, CD8 or CD14 positive cells. Scale bar = 5 μm. (D–E) Frequency of CD25 (D) and CD69 (E) expressing T lymphocytes in unstimulated and ConA-stimulated PBMC cultures in the absence or presence of increasing concentrations of BIM5078. (F–G) Percentage of CD25 (F) and CD150 (G) positive monocytes in unstimulated and LPS-stimulated cultures at increasing concentrations of BIM5078. (H–K) The same as in (D–G) reporting T lymphocyte (H–I) and monocyte (J–K) activation after BI6015 treatment. (L) Heatmap showing differentially expressed genes in untreated vs. BI6015 treated PBMC. Highlighted are genes associated with regulation of immune cell activation. (M – N) ConA-induced T cell proliferation of human PBMC (M) and mouse splenocytes (N) after exposure to increasing concentrations of BIM5078 (M) or BI6015 (N). (O) Ex-vivo T cell proliferation in a spleen culture from a MOG_{35-55} peptide immunized mouse when exposed in vitro to vehicle or BIM5078. (P) EAE expression in mice orally treated with HNF4α inhibitors (BIM5078 n = 9 or BI6015 n = 8) or vehicle (n = 10) from day 7 post immunization. Bars represent SEM. (Q–R) Ex vivo proliferation of MOG_{35-55} -specific T cells from the spleens (Q) or draining lymph nodes (R) of BIM5078-, BI6015- or vehicle-treated EAE mice (n = 5 animals/group). Representative data of one out of 2–6 independent experiments are shown. Statistical analysis: Student *t*-test in (D-K, M, N) and linear regression in (O–R). In (P) differences between slopes were analyzed from day 17 post immunization. *p-value <0.05, **p-value <0.01, ***p-value <0.001, ****p-value <0.0001. See also Figs. S1 and S2 and Supplementary Table 1.

exposed for 4 h to BI6015 or to vehicle evidenced that the compound induced higher expression of genes inhibiting immune cell activation, such as MEFV [23], CD8b and LYZ genes [24], while downregulating LEPR [25], CD69, CD83 [26], CLEC7A [27] and HLADRB6 and other positive regulators of immune function (Fig. 1L, Table S1). Indeed, exposure to HNF4α antagonists significantly reduced ConA-induced T cell proliferation in human (Fig. 1M) and mouse cultures (Fig. 1N). To verify whether HNF4α antagonism could interfere with antigen-driven activation, we immunized C57BL6 mice with the encephalitogenic MOG_{35-55} peptide, recovered the spleens and measured the proliferation of antigen-specific T cells ex vivo in absence or presence of BIM5078. HNF4α antagonism inhibited in vitro MOG_{35-55} peptide-specific T cell proliferation (Fig. 1O). These results offered the rationale for in vivo administration of HNF4α antagonists in the experimental model of MS, the EAE. Daily oral administration of HNF4α inhibitors from day 7 post immunization before any clinical manifestations significantly ameliorated disease severity and demonstrated higher efficacy for BI6015 than BIM5078 (Fig. 1P and S2). Consistently, ex vivo T cell responses in the spleens (Fig. 1Q) and draining lymph nodes(Fig. 1R) of the three groups of animals indicated that in vivo HNF4α antagonism inhibited MOG_{35-55} peptide-specific T cell responses, with a stronger effect mediated by BI6015 (Fig. 1Q-R).

Overall, these results indicated that HNF4α activity supported innate and adaptive immunity in vitro and in vivo, and identified novel compounds, BIM5078 and BI6015, targeting HNF4α for the regulation of neuroinflammation.

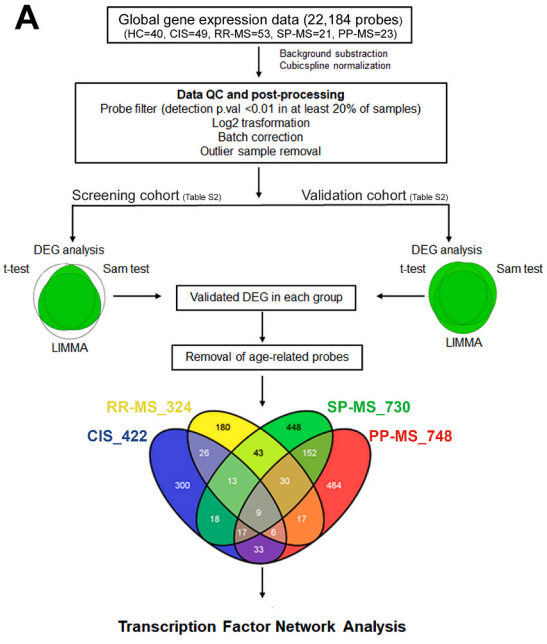

B

	SP1			HNF4α			c-myc		
	Seed nodes	z-score	p-Value	Seed nodes	z-score	p-Value	Seed nodes	z-score	p-Value
CIS	98	3,02	1,11E-03	82	2,56	5,51E-03	72	2,28	1,37E-02
RR-MS	71	2,92	1,56E-03	66	2,73	3,04E-03	58	2,44	8,33E-03
PP-MS	180	2,81	2,36E-03	200	3,11	8,09E-04	166	2,60	4,77E-03
SP-MS	175	3,04	9,91E-04	166	2,89	1,70E-03	141	2,49	6,81E-03

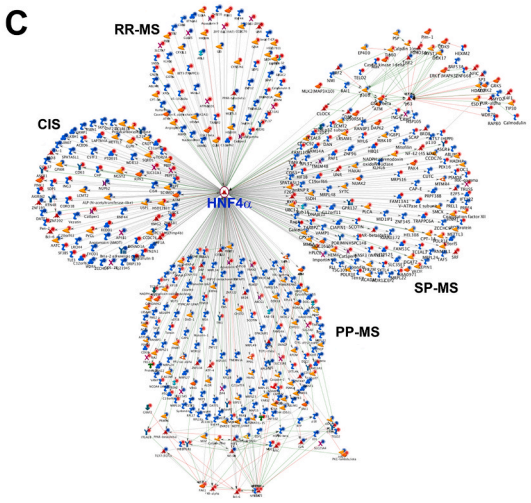

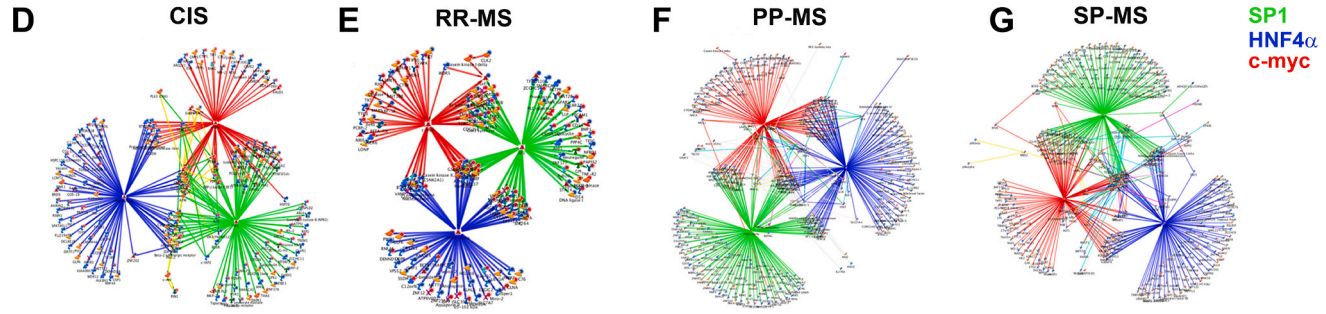

Fig. 2. HNF4α, SP1 and c-myc are common transcription factor network hubs in immune signatures of CIS and MS subjects. (A) Flow chart for the study of PBMC transcriptomes from healthy and diseased subjects. Gene expression data relative to healthy controls, CIS, RR-MS, SP-MS and PP-MS patients were collected. Raw intensities were background-subtracted using nec function in LIMMA package, normalized and filtered. Then, 11,184 probes were log2 transformed and subjected to batch correction using ComBat package. The samples were divided into screening and validation cohorts (ratio ~ 50:50) and each diseased group was compared to the healthy population. To identify DEG three parallel statistical methods were applied: Welch *t*-test (p-value <0.05), Significant Analysis of Microarrays (fdr <0.2) and LIMMA (p-value <0.05). A validated DEG was the one that passed at least two tests in the screening group and at least one test in the validation group. Since PP- and SP-MS group included older subjects than CIS and RR-MS patients, genes correlating with aging were identified by measuring the Spearman's rank correlation between the age and expression level in the healthy group, and removed from the list of the validated DEG. Venn Diagram shows unique and overlapping age-corrected validated DEG. Finally, DEG lists were used for Transcription Factor Network Analysis (TFNA). (B) Significant transcription factor network hubs at each disease stage. (C) A graphical depiction of HNF4α network in all disease lists. HNF4α present at the center of the network is linked to DEG (nodes) appearing in the distinct CIS, RR-MS, PP-MS and SP-MS signatures. (D–G) HNF4α (blue), SP1 (green) and c-myc (red) network interactions in CIS (D), RR-MS (E), PP-MS (F) and SP-MS (G) transcriptomes.

3.2. HNF4α, SP1 and c-myc are transcription factor network hubs in MS blood transcriptomes

MS is a neurological disorder characterized by heterogeneity in clinical courses, manifestations and histopathological findings [28]. CIS represent the first clinical episode of an inflammatory demyelinating disorder suggestive of MS. Most CIS will develop RR-MS, characterized by clinical and inflammatory attacks followed by periods of recovery and stability. With time, most RR-MS subjects will evolve to SP-MS, with advancing neurological impairment in absence of recognizable relapses. A small fraction of MS subjects experience worsening of neurologic function from the onset and are thus defined PP-MS [29]. We analyzed PBMC transcriptomes relative to 40 healthy subjects, 49 CIS, 53 RR-MS, 21 SP-MS and 23 PP-MS patients (Table S2, ArrayExpressID E-MTAB-11415), and applied a semi-automated pipeline in R Bioconductor platform to perform preprocessing and differential expression analysis (Fig. 2A). Towards the identification of differentially expressed genes, samples were divided into screening and validation cohorts (ratio ~ 50:50) according to specific clinical and demographic criteria (Table S2) and transcriptomes from each disease group were compared to those from the healthy population. We used three parallel statistical methods to identify the differentially expressed genes (DEG): Welch *t*-test (p-value <0.05), Significant Analysis of Microarrays (FDR <0.2) and LIMMA (p-value <0.05). A validated differentially expressed gene (DEG) was the one that passed at least two tests in the screening group and at least one test in the validation group. As PP-MS and SP-MS groups included older subjects than CIS and RR-MS patients, probes correlating with aging were identified by measuring the Spearman's rank correlation between age and expression level in the healthy group and removed from the list of the validated DEG. Thus, we obtained 4 distinct lists of DEG which were normalized against the healthy population and validated in two comparisons on independent screening and validation samples (Fig. 2A). The CIS, RR-MS, SP-MS and PP-MS signatures comprised 422, 324, 730, 748 probes respectively, and partially overlapped among the distinct disease stages (Fig. 2A), indicating unique and shared transcriptional dysregulations at distinct stages of disease. To define transcriptional regulators of differential expression in MS, we performed transcription factor network analysis (TFNA), which maps possible interactions between DEG and candidate TF, thus generating interactomes for each TF passing statistical significance. TFNA analysis revealed three significant transcription factor network hubs associated with the transcriptional signatures of CIS and all MS forms and centered around HNF4α, SP1 and c-myc (Fig. 2B). A graphical depiction of HNF4α network in all disease groups is shown in Fig. 2C, where HNF4α is at the center of the network and linked to DEG (nodes) appearing in the distinct CIS, RR-MS, PP-MS and SP-MS signatures. Interestingly, the analysis of the network for the three TFs at each stage of disease showed that the three TF networks (HNF4α in blue, c-myc in red, SP1 in green) were not independent one from the other but that several DEG were positioned at the interface and contacted by more than one TF, suggesting coregulation of differential expression in MS (Fig. 2D–G). Thus, the analysis of human immune cell transcriptomes in health and under distinct stages of disease coupled with the reconstruction of the significant transcriptional networks linked to differential expression highlighted three key interactomes in all MS signatures based on HNF4α, SP1 and c-myc.

3.3. HNF4α, SP1 and c-myc triad is higher in MS immune cells, boosted by activation and further enhanced by environmental MS risk factors

To validate in silico data about interaction among HNF4α, SP1 and c-myc networks in immune cells, we initially measured nuclear protein levels of these TFs in PBMC from healthy subjects under resting and stimulated conditions. As shown in Fig. 3 A-D, the low levels of TFs and the absence of colocalization with HNF4α detected in resting cells changed and significantly augmented upon T cell (Fig. 3A and C) or monocyte (Fig. 3B and D) stimulation, indicating that immune cell activation regulated TF protein levels and led to their colocalization.

Cigarette smoke and low levels of vitamin D are known risk factors for MS [30]. We checked whether culture media conditioned with cigarette smoke (CS) or added with the biologically active form of vitamin D3 called 1α,25-dihydroxyvitamin D3 (aVit D3) modulated in vitro the activation of myelin-reactive T cells isolated from EAE mice. Conventional cell culture media contain little vitamin D due to serum dilution and thus reproduce the low vitamin D condition. While the addition to culture media of physiological plasma levels of aVit D3 [31] restricted T cell function (Fig. 3E), non toxic levels of CS-conditioned media enhanced MOG-specific T cell proliferation (Fig. 3F). Similarly, physiological aVit D3 reduced the activation of human T lymphocytes (Fig. 3G and H), whereas CS media showed the opposite effect (Fig. 3I and J). Importantly, activation of T lymphocytes at low levels of Vit D as in control media or in the presence of CS was associated with significantly higher nuclear levels of HNF4α, SP1 and c-myc compared to aVit D3-conditioned media or control media respectively (Fig. 3K).

Finally, we verified TF protein expression ex vivo in PBMC from MS and healthy subjects and found higher levels of HNF4α and SP1 in MS cells compared to control cells, while c-myc protein was similarly expressed in healthy and MS immune cells (Fig. 3L-O). High-resolution nuclear mapping of HNF4α and SP1 by super-resolution microscopy confirmed major TF expression and colocalization in MS cells (Fig. 3P). Thus immune cell activation and dysimmune condition under pathology were characterized by alterations in TF expression and colocalization.

3.4. HNF4α, SP1 and c-myc exert non-synergic, interdependent transcriptional control of immunity in vitro and in vivo

A biochemical study conducted in cancer cell lines suggested that competitive interaction of HNF4α, SP1 and c-myc may take place at gene promoters, depend on c-myc levels and skew cell function [32]. To define the outcome of TF interaction on immune cell activation, we performed in vitro experiments on human PBMC with compounds targeting HNF4α, SP1 and c-myc. We used BI6015 for HNF4α blockade and WP631 (a DNA intercalating compound at SP1 binding sites [33,34]) for SP1 inhibition. As no direct c-myc antagonists are currently available, we used OTX015 which downregulates c-myc expression by targeting bromodomain and extraterminal domain proteins [35]. As control experiment, we checked whether the inhibitors altered TF expression in unstimulated and ConA- or LPS-stimulated human immune cells. While HNF4α antagonism at the ligand-binding domain by BI6015 did not change any TF expression in resting and activated T lymphocytes (Fig. S3A) and monocytes (Fig. S3B), SP1 and c-myc inhibition hampered specifically target levels in activated cells (Figs. S3A–B). Next, we tested the effects of dual TF inhibition on immune cell activation by flow cytometry. Fig. 4 displays ConA- or LPS-mediated induction of activation markers on T cells (Fig. 4A and C) or monocytes (Fig. 4B and D) respectively and 100% indicates maximal induction achieved in absence of TF inhibitors. Interestingly, HNF4α inhibitor alone was more efficient in blocking the activation of T lymphocytes (Fig. 4A) and monocytes (Fig. 4B) than SP1 antagonist alone or their combination, indicating that the action of the two TFs was not synergic and that the effect of HNF4α antagonism on immune cell function partly relied on SP1 transcriptional activity. Though c-myc inhibition alone did not impair T lymphocyte (black line, Fig. 4C) and monocyte activation (black line, Fig. 4D), it weakened the immunosuppressive action of HNF4α inhibitor and completely blocked the one of the SP1 inhibitor (red line, Fig. 4C and D), suggesting that immune cell activation depended on HNF4α and SP1 transcriptional activity only if c-myc levels were high. Similar to the in vitro results, HNF4α and SP1 inhibitors ameliorated EAE expression even when administered in a therapeutic setup three days after disease onset, with a stronger effect displayed by HNF4α inhibitor, but their combination did not have any synergistic action (Fig. 5A-B and S4A). In harmony with in vivo observations, ex

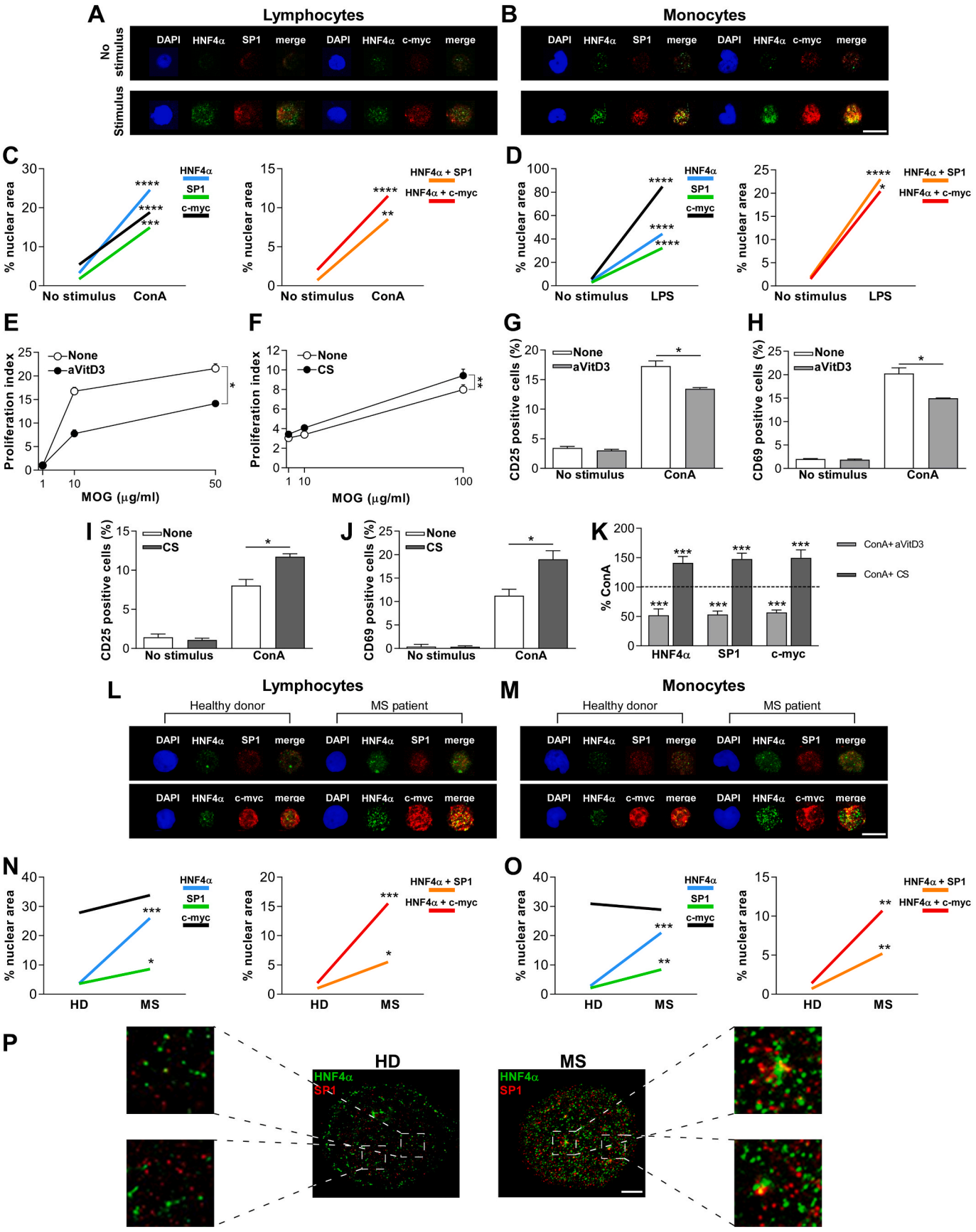

(caption on next page)

Fig. 3. HNF4α, SP1 and c-myc interact but do not exert synergistic activity on immune cell activation (A–D) Representative confocal imaging for HNF4α (green), SP1 or c-myc (red) in nuclei of lymphocytes (A) and monocytes (B) from healthy donors in resting (upper panels) or stimulated conditions (lower panels) and relative quantifications (C–D). Nuclei were stained with DAPI (blue). (C–D) Nuclear levels of transcription factors (left panels) and colocalization between HNF4α and SP1 or c-myc (right panels) in resting, ConA- (C) or LPS- (D) stimulated PBMC cultures. (E–F) Ex-vivo T cell proliferation in splenocyte cultures from MOG_{35-55} peptide immunized mice after in vitro exposure to control media or aVitD3- (E)/CS (F)-conditioned media. Data are reported as mean proliferation index in splenocyte cultures from n = 4 (E) or n = 5 (F) EAE mice, and error bars represent SEM. (G–J) Percentage of CD25 (G,I) and CD69 (H,J) expressing T lymphocytes exposed to control media, aVitD3 (G–H) or CS (I–J) in resting or ConA-stimulated PBMC cultures. (K) Nuclear levels of HNF4α, SP1 and c-myc in ConA-stimulated PBMC cultures exposed to aVitD3 (light grey columns) or CS (dark grey colums). Data are reported as percentage of values obtained in control cultures exposed to ConA only. (L–O) Representative confocal images showing HNF4α (green), SP1 (red; upper panels) and c-myc (red; lower panels) protein expression in lymphocytes (L) and monocytes (M) from healthy donors (n = 5, left panels) or MS patients (n = 4, right panels) and relative quantifications (N–O). (P) Representative super-resolution microscopy images of HNF4α (green) and SP1 (red) in cells from a healthy subject (left) or MS patient (right). Representative data of one out of 3 in (C–D) or 3–10 in (G–K). In (K), the sum of 3 independent experiments is reported and error bars represent SEM. Scale bars = 10 μm in (A-B, L-M), 20 μm in (P). Statistical analysis: linear regression in (E–F) and Student *t*-test in (C-D, J-K, N–O. *p-value <0.05, **p-value <0.01, ***p-value <0.001, ****p-value <0.0001. See also Fig. S3.

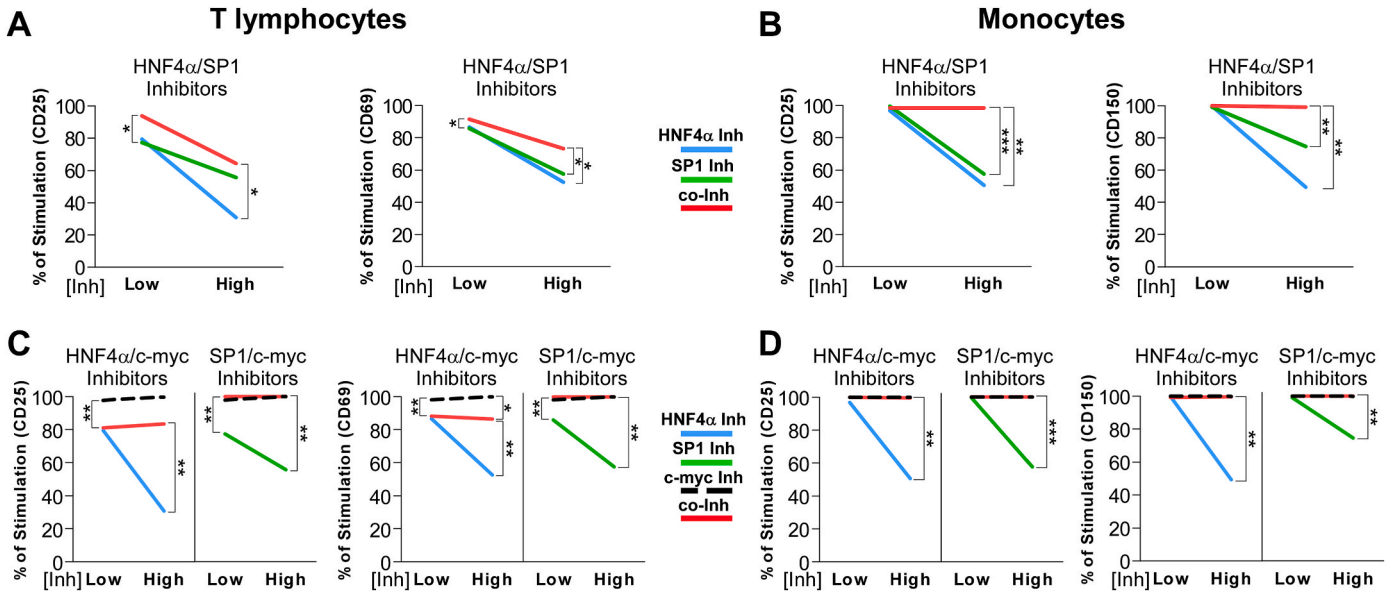

Fig. 4. Effects of TF inhibitors on immune cell activation. (A–D) Expression of activation markers on T lymphocytes (A,C) and monocytes (B,D) in PBMC cultures stimulated with inhibitors for HNF4α (BI6015, light blue lines), SP1 (WP631, green lines), c-myc (OTX015, black lines) or control media. Red lines report combination of inhibitors. 100% indicates maximal induction achieved in absence of TF inhibitors and data are reported as percentage with respect to control condition. Concentration used were: 0,06 μM (low) and 0,6 μM (high) for BI6015, 0,01 μM (low) and 0,1 μM (high) for WP631, 100 nM (low) and 100 μM (high) for OTX015. Representative data of one out of 3 independent experiments are shown. Statistical analysis: Student *t*-test. *p-value <0.05, **p-value <0.01, ***p-value <0.001.

vivo encephalitogenic T cell responses were mostly reduced in EAE mice treated with SP1 or HNF4α inhibitors alone (Fig. 5C and D). Similarly, HNF4α inhibitor displayed the maximal therapeutic effect in the EAE model when given alone rather than in combination with c-myc inhibitor, which also significantly ameliorated disease course when given alone (Fig. 5E-F and S4B). Interestingly, treatment discontinuation after day 33 post immunization did not lead to disease worsening, indicating a long-lasting therapeutic effect (Fig. S4C). Ex vivo encephalitogenic T cell responses in the spleen and lymph nodes were mostly affected in mice treated with HNF4α inhibitor alone (Fig. 5G and H).

In summary, HNF4α, SP1 and c-myc were coexpressed in immune cells but immune cell activation, the generation of myelin-reactive T cell responses and the expression of experimental neuroinflammation depended strongly on HNF4α mainly in the context of normal SP1 and c-myc function.

4. Discussion

4.1. *HNF4α regulates immunity and neuroinflammation*

Despite previous work showing detectable HNF4α transcripts in immune cells [36], no information was available about the role of this TF in immunity. Here we report that HNF4α is expressed by immune cells where it supports activation, proliferation and cytokine release, and that its inhibition reduces the generation of myelin-reactive T cells in lymphoid organs and ameliorates disease severity in the experimental model of multiple sclerosis. Since HNF4α is known to be implicated in other pathological conditions, such as hepatitis B and liver cancer [37, 38], many efforts have been made to develop compounds inhibiting HFN4 α activity. BIM5078 is a potent HNF4α antagonist that directly binds HNF4α ligand-binding pocket and modulates the expression of known HNF4α target genes [20]. However, in vivo pharmacokinetic studies indicate low plasma stability, moderate microsomal stability and low solubility for this compound. Among structural analogs of BIM5078, BI6015 exerts potent and specific HNF4α inhibition and a better pharmacokinetic profile [20]. Differently from a published study showing drug effects on cancer cell lines at high concentration (>5 μM) [20], in our in vitro system of primary immune cells very low, non toxic concentrations (0,3–0,6 μM) of HNF4α antagonists were sufficient to inhibit activation and cytokine production by human T cells and monocytes and reduced overall mouse and human T cell proliferation. Indeed, HNF4α inhibition downregulated genes supporting immune cell activation in human PBMC, while upregulating negative regulators of immune function. A report combining ChIP assays with expression profiling after HNF4α RNA interference and protein binding microarrays in HepG2 cells identified several genes involved in immune response as direct targets of HNF4α [39], some of which (e.g. MAF, GM2A and HNMT) have dysregulated higher expression in MS PBMC compared to healthy

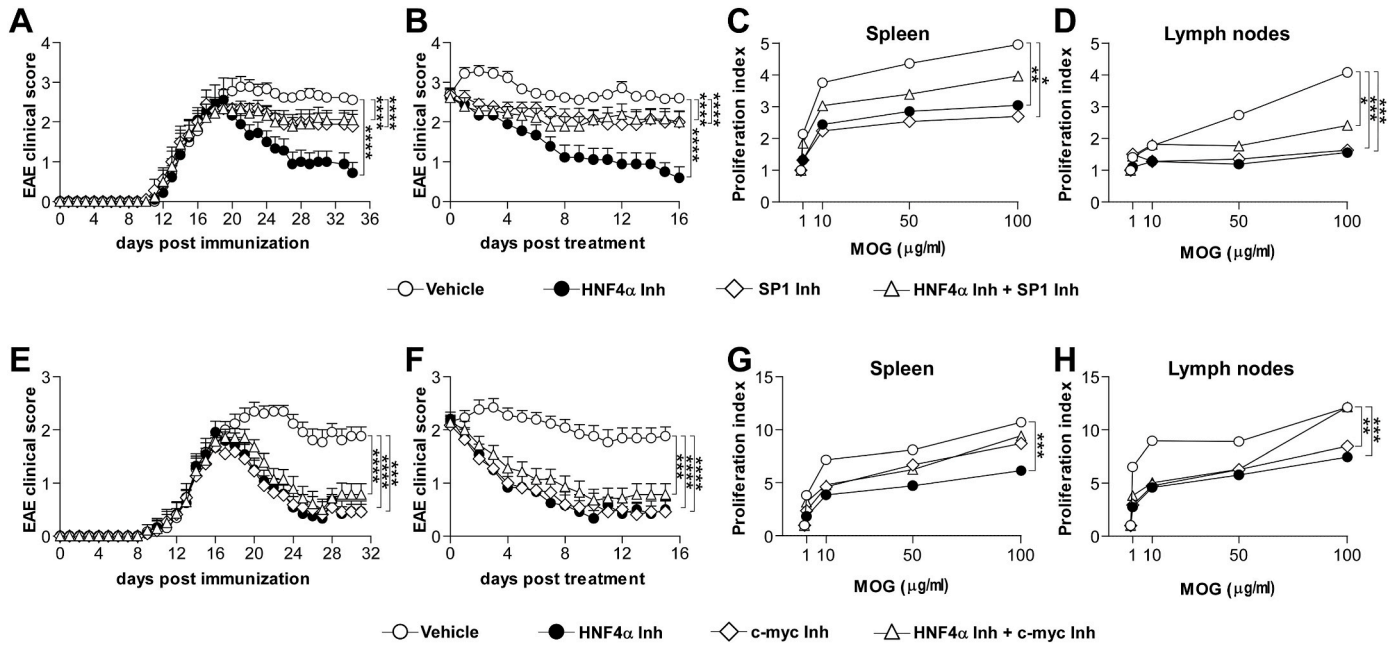

Fig. 5. Interdependence of HNF4α, SP1 and c-myc in the control of CNS autoimmunity (A–B) EAE progression in mice starting daily oral treatment with HNF4α inhibitor (n = 9), SP1 inhibitor (n = 9), both inhibitors (n = 9) or vehicle (n = 9) three days after disease onset. (C–D) Ex vivo proliferation of MOG_{35-55}-specific T cells from the spleens (C) or draining lymph nodes (D) of EAE mice treated with TF inhibitors (n = 4/group). (E–F) EAE expression in mice treated with HNF4α inhibitor (n = 12), c-myc inhibitor (n = 11), both inhibitors (n = 14) or vehicle (n = 13). (G–H) Ex vivo proliferation of MOG_{35-55}-specific T cells from the spleens (G) or draining lymph nodes (H) of EAE mice treated with TF inhibitors or vehicle (n = 5/group). Graphs in (A) and (E) show mean clinical scores and SEM from day of immunization, graphs in (B) and (F) depict mean clinical score and SEM according to treatment duration. Statistical analysis was performed using linear regression. In (A) and (E) differences between slopes were analyzed from day 18 or 17 post immunization respectively.*p-value <0.05, **p-value <0.01, ***p-value <0.001, ****p-value <0.0001. See also Fig. S4.

controls [7,8]. This evidence suggests that HNF4α antagonism may represent an appropriate pharmacological strategy to counterregulate immune dysregulations in MS and treat the disease. Consistently, we observed that in vivo administration of HNF4α antagonists reduced EAE severity and T cell responses to the encephalitogenic MOG peptide, with BI6015 being more potent than BIM5078. However, we cannot exclude that systemic administration of these small molecules may affect other compartments in addition to peripheral immunity. Overall, these results affirm the existence of a novel transcriptional regulator supporting the activation of innate and adaptive immune responses, and of a novel class of immunomodulatory compounds for the treatment of CNS autoimmunity.

4.2. *HNF4α is a part of a complex TF network in MS*

A published gender-based analysis of PBMC transcriptomes underlined epigenetic and transcriptional processes as common dysregulated themes associated with the relapsing-remitting form of MS, proposed a network of epigenetic regulators associated with differential expression in MS, and validated the role of the transcription factor SP1 in sustaining T cell proliferation and experimental neuroinflammation [6]. Interestingly, HNF4α was part of that epigenetic network and critically connected to the greatest number of differentially expressed genes in female and male MS PBMC [6]. In the current study, when applying network biology to immune transcriptomes dysregulated at different courses or stages of MS, we identified three key interactomes in all disease signatures based on SP1, HNF4α and c-myc. Notably, we provided the first evidence that HNF4α and SP1 were present in lymphocytes and monocytes and enriched in MS nuclei, while c-myc levels were already high in healthy cells. Interestingly, T cell and monocyte activation in our PBMC cultures led to the increase of nuclear TF and their colocalization. MS is a complex disorder characterized by immune dysregulation [40,41] and contributed partly by genetic predisposition, mostly by environmental triggers [42]. Among MS risk factors we focused our attention on cigarette smoke and low vitamin D levels [30], both known to regulate immunity [43,44]. Conventional cell culture media contain little vitamin D due to serum dilution and thus reproduce the low vitamin D condition. Notably, activation of human immune cells, proliferation of encephalitogenic T cells and TF expression were dramatically reduced under physiological plasma concentrations of vitamin D, indicating that low vitamin D favours immune reactivity and high TF levels. Further, our in vitro and ex vivo activation assays on human and mouse immune cells reproducibly showed that media conditioned with non-toxic concentrations of cigarette smoke promoted immune cell activation, T cell proliferation and the expression of the three TFs.

Overall, we demonstrate a direct correlation between known MS risk factors, immune responses and levels of TF regulating immunity and differential immune expression at all stages of MS.

4.3. *Interdependence of HNF4α, SP1 and c-myc in the control of CNS autoimmunity*

Our transcriptomic and network biology observations pointed to the existence of a complex transcriptional basis and control among distinct courses and stages of MS. This is a relevant issue for MS therapy, as most of the currently approved disease-modifying therapies demonstrated efficacy in relapsing-remitting but not progressive MS. Indeed, recent reports suggest that progressive forms of multiple sclerosis present with distinct immunological and transcriptional alterations [7,8,45], which may allow the specific classification of progressive MS from relapsing-remitting MS with high accuracy by machine leaning algorithms [9]. On the other hand, the identification of transcriptional master regulators shared by all MS stages may support the development of therapies with potential efficacy also in progressive MS. Our in silico analyses highlighted in all MS stages that the three TF-based interactomes were not independent one from the other but shared part of the

dysregulated transcriptome, suggesting possible coregulations of differential expression. Indeed, in vitro experiments demonstrated that the combined action of HNF4α and SP1 inhibitors was not synergistic and that the effect of HNF4α antagonism on immune cell function partly relied on SP1 transcriptional activity. Though c-myc inhibition alone did not impair T lymphocyte and monocyte activation, indicating that c-myc is not regulating immune cell function directly, it weakened the immunosuppressive action of HNF4α inhibitor and completely blocked that of the SP1 inhibitor. Similar results were observed when we tested TF inhibitors in combination in vivo and measured ex vivo proliferation of myelin-rective T cells. The evidence that the c-myc inhibitor OTX015 did not exert suppression of T cell and monocyte activation in vitro but inhibited encephalitogenic T cell expansion in vivo suggests a direct mode of action on other cell types or functions relevant for the generation and expansion of autoreactive T lymphocytes [46]. It is known that OTX015 downregulates c-myc expression by targeting BET proteins [47]. BET inhibitors may impact expression of additional genes as BET proteins regulate gene transcription via multiple mechanisms, including chromatin remodeling, transcription factor recruitment and stability, transcription and splicing integration [48]. Thus, we cannot exclude that, in addition to c-myc, other OTX015 targets contribute to OTX015 action. Still, our data indicate that each TF inhibitor does not alter the expression of the two other TFs, thus excluding a downstream effect on the levels of other master regulators of (neuro)inflammation. Based on these findings, we hypothesize an activation model for immune cells interdependent on the three identified master regulators, which deserves future investigation also in consideration of possible role of the TF (and of the TF inhibitors) on distinct immune cell subsets.

Notably, the administration of TF inhibitors had substantial effects on EAE progression. We have previously shown that SP1 inhibition before EAE onset reduced clinical severity [6]. Here we confirmed its efficacy even when provided after EAE onset during the chronic phase of disease. In the same experimental set up, HNF4α and c-myc inhibitors displayed the most remarkable therapeutic effects in chronic EAE, supporting the application of these epigenetic drugs to the treatment of MS. The combination therapy experiments, however, confirmed the complex interdependence of the action of the three transcriptional master regulators and underscored a non synergistic effect of the drugs on EAE expression.

Overall, we identify HNF4α, c-myc and SP1 as master regulators of transcriptional dysregulation shared by all MS courses, with two of them, HNF4α and SP1, displaying higher nuclear localization in MS blood cells. Small compounds targeting the three TFs are already available and showed great efficacy in the treatment of chronic neuroinflammation. These results support pharmacological targeting of single TF in people with distinct disease courses, including progressive MS.

Funding

The study was funded by Healthcare business of Merck KGaA, Darmstadt, Germany (CrossRef Funder ID: 10.13039/100009945 to CF) as part of an alliance with Ospedale San Raffaele and Italian Ministry of Health (RF-2011-02349698, RF-2018-12367731 to CF).

Author contributions

Conceptualization: C.F. Investigation: E.C., M.D.D., R.M., V.M.M., C. B., N.S., D.M. Formal Analysis: E.C., M.D.D., R.M., C.F. Resources: F.M., L.M., V.M., G.C., C.F. Writing: E.C., V.M.M., C.F. Visualization: E.C., R. M. Supervision: C.F. Funding Acquisition: C.F.

Declaration of competing interest

The authors declare no competing interests related to the manuscript.

Acknowledgments

The authors thank Sundararajan Srinivasan and Chiara Govi for preliminary experiments and all participants who donated blood for this study.

Appendix A. Supplementary data

Supplementary data to this article can be found online at https://doi.org/10.1016/j.jaut.2023.103053.

References

[1] F.M. Sladek, W.M. Zhong, E. Lai, J.E. Darnell Jr., Liver-enriched transcription factor HNF-4 is a novel member of the steroid hormone receptor superfamily, Genes Dev. 4 (1990) 2353–2365.
[2] H.H. Lau, N.H.J. Ng, L.S.W. Loo, J.B. Jasmen, A.K.K. Teo, The molecular functions of hepatocyte nuclear factors - in and beyond the liver, J. Hepatol. 68 (2018) 1033–1048.
[3] A.D. Petrescu, R. Hertz, J. Bar-Tana, F. Schroeder, A.B. Kier, Ligand specificity and conformational dependence of the hepatic nuclear factor-4alpha (HNF-4alpha), J. Biol. Chem. 277 (2002) 23988–23999.
[4] R. Hertz, J. Magenheim, I. Berman, J. Bar-Tana, Fatty acyl-CoA thioesters are ligands of hepatic nuclear factor-4alpha, Nature 392 (1998) 512–516.
[5] M.G. Holloway, E.V. Laz, D.J. Waxman, Codependence of growth hormone-responsive, sexually dimorphic hepatic gene expression on signal transducer and activator of transcription 5b and hepatic nuclear factor 4alpha, Mol. Endocrinol. 20 (2006) 647–660.
[6] R. Menon, M. Di Dario, C. Cordiglieri, S. Musio, L. La Mantia, C. Milanese, A.L. Di Stefano, M. Crabbio, D. Franciotta, R. Bergamaschi, R. Pedotti, E. Medico, C. Farina, Gender-based blood transcriptomes and interactomes in multiple sclerosis: involvement of SP1 dependent gene transcription, J. Autoimmun. 38 (2012) J144–J155.
[7] S. Srinivasan, M. Di Dario, A. Russo, R. Menon, E. Brini, M. Romeo, F. Sangalli, G. D. Costa, M. Rodegher, M. Radaelli, L. Moiola, D. Cantarella, E. Medico, G. Martino, R. Furlan, V. Martinelli, G. Comi, C. Farina, Dysregulation of MS risk genes and pathways at distinct stages of disease, Neurol. Neuroimmunol. Neuroinflammation 4 (2017) e337.
[8] S. Srinivasan, M. Severa, F. Rizzo, R. Menon, E. Brini, R. Mechelli, V. Martinelli, P. Hertzog, M. Salvetti, R. Furlan, G. Martino, G. Comi, E.M. Coccia, C. Farina, Transcriptional dysregulation of interferome in experimental and human multiple sclerosis, 017-09286-y, Sci. Rep. 7 (2017) 8981.
[9] M. Acquaviva, R. Menon, M. Di Dario, G. Dalla Costa, M. Romeo, F. Sangalli, B. Colombo, L. Moiola, V. Martinelli, G. Comi, C. Farina, Inferring multiple sclerosis stages from the blood transcriptome via machine learning, Cell. Rep. Med. 1 (2020), 100053.
[10] A. Compston, Making progress on the natural history of multiple sclerosis, Brain 129 (2006) 561–563.
[11] H.L. Ko, Z. Zhuo, E.C. Ren, HNF4alpha combinatorial isoform heterodimers activate distinct gene targets that differ from their corresponding homodimers, Cell Rep. 26 (2019) 2549–2557.e3.
[12] R.T. Holman, S.B. Johnson, E. Kokmen, Deficiencies of polyunsaturated fatty acids and replacement by nonessential fatty acids in plasma lipids in multiple sclerosis, Proc. Natl. Acad. Sci. U.S.A. 86 (1989) 4720–4724.
[13] E. Colombo, C. Cordiglieri, G. Melli, J. Newcombe, M. Krumbholz, L.F. Parada, E. Medico, R. Hohlfeld, E. Meinl, C. Farina, Stimulation of the neurotrophin receptor TrkB on astrocytes drives nitric oxide production and neurodegeneration, J. Exp. Med. 209 (2012) 521–535.
[14] W.I. McDonald, A. Compston, G. Edan, D. Goodkin, H.P. Hartung, F.D. Lublin, H. F. McFarland, D.W. Paty, C.H. Polman, S.C. Reingold, M. Sandberg-Wollheim, W. Sibley, A. Thompson, S. van den Noort, B.Y. Weinshenker, J.S. Wolinsky, Recommended diagnostic criteria for multiple sclerosis: guidelines from the International Panel on the diagnosis of multiple sclerosis, Ann. Neurol. 50 (2001) 121–127.
[15] M. Reimers, V.J. Carey, Bioconductor: an open source framework for bioinformatics and computational biology, Methods Enzymol. 411 (2006) 119–134.
[16] G.K. Smyth, Linear models and empirical bayes methods for assessing differential expression in microarray experiments, Article3, Stat. Appl. Genet. Mol. Biol. 3 (2004).
[17] W. Shi, A. Oshlack, G.K. Smyth, Optimizing the noise versus bias trade-off for Illumina whole genome expression BeadChips, Nucleic Acids Res. 38 (2010), e204.
[18] W.E. Johnson, C. Li, A. Rabinovic, Adjusting batch effects in microarray expression data using empirical Bayes methods, Biostatistics 8 (2007) 118–127.
[19] M. Heilemann, S. van de Linde, M. Schuttpelz, R. Kasper, B. Seefeldt, A. Mukherjee, P. Tinnefeld, M. Sauer, Subdiffraction-resolution fluorescence imaging with conventional fluorescent probes, Angew. Chem., Int. Ed. Engl. 47 (2008) 6172–6176.
[20] A. Kiselyuk, S.H. Lee, S. Farber-Katz, M. Zhang, S. Athavankar, T. Cohen, A. B. Pinkerton, M. Ye, P. Bushway, A.D. Richardson, H.A. Hostetler, M. Rodriguez-Lee, L. Huang, B. Spangler, L. Smith, J. Higginbotham, J. Cashman, H. Freeze, P. Itkin-Ansari, M.I. Dawson, F. Schroeder, Y. Cang, M. Mercola, F. Levine,

HNF4alpha antagonists discovered by a high-throughput screen for modulators of the human insulin promoter, Chem. Biol. 19 (2012) 806–818.
[21] M. Di Dario, E. Colombo, C. Govi, D. De Feo, M.J. Messina, M. Romeo, F. Sangalli, L. Moiola, M. Rodegher, G. Martino, V. Martinelli, G. Comi, C. Farina, Myeloid cells as target of fingolimod action in multiple sclerosis, Neurol. Neuroimmunol. Neuroinflammation 2 (2015) e157.
[22] C. Farina, D. Theil, B. Semlinger, R. Hohlfeld, E. Meinl, Distinct responses of monocytes to Toll-like receptor ligands and inflammatory cytokines, Int. Immunol. 16 (2004) 799–809.
[23] M. Centola, G. Wood, D.M. Frucht, J. Galon, M. Aringer, C. Farrell, D.W. Kingma, M.E. Horwitz, E. Mansfield, S.M. Holland, J.J. O'Shea, H.F. Rosenberg, H. L. Malech, D.L. Kastner, The gene for familial Mediterranean fever, MEFV, is expressed in early leukocyte development and is regulated in response to inflammatory mediators, Blood 95 (2000) 3223–3231.
[24] J.M. Taube, G.D. Young, T.L. McMiller, S. Chen, J.T. Salas, T.S. Pritchard, H. Xu, A. K. Meeker, J. Fan, C. Cheadle, A.E. Berger, D.M. Pardoll, S.L. Topalian, Differential expression of immune-regulatory genes associated with PD-L1 display in melanoma: implications for PD-1 pathway blockade, Clin. Cancer Res. 21 (2015) 3969–3976.
[25] R. Wei, Y. Hu, F. Dong, X. Xu, A. Hu, G. Gao, Hepatoma cell-derived leptin downregulates the immunosuppressive function of regulatory T-cells to enhance the anti-tumor activity of CD8+ T-cells, Immunol. Cell Biol. 94 (2016) 388–399.
[26] E. Zinser, R. Naumann, A.B. Wild, J. Michalski, A. Deinzer, L. Stich, C. Kuhnt, A. Steinkasserer, I. Knippertz, Endogenous expression of the human CD83 attenuates EAE symptoms in humanized transgenic mice and increases the activity of regulatory T cells, Front. Immunol. 10 (2019) 1442.
[27] D. Duluc, H. Joo, L. Ni, W. Yin, K. Upchurch, D. Li, Y. Xue, P. Klucar, S. Zurawski, G. Zurawski, S. Oh, Induction and activation of human Th17 by targeting antigens to dendritic cells via dectin-1, J. Immunol. 192 (2014) 5776–5788.
[28] R. Dobson, G. Giovannoni, Multiple sclerosis - a review, Eur. J. Neurol. 26 (2019) 27–40.
[29] F.D. Lublin, S.C. Reingold, J.A. Cohen, G.R. Cutter, P.S. Sorensen, A.J. Thompson, J.S. Wolinsky, L.J. Balcer, B. Banwell, F. Barkhof, B. Bebo Jr., P.A. Calabresi, M. Clanet, G. Comi, R.J. Fox, M.S. Freedman, A.D. Goodman, M. Inglese, L. Kappos, B.C. Kieseier, J.A. Lincoln, C. Lubetzki, A.E. Miller, X. Montalban, P.W. O'Connor, J. Petkau, C. Pozzilli, R.A. Rudick, M.P. Sormani, O. Stuve, E. Waubant, C. H. Polman, Defining the clinical course of multiple sclerosis: the 2013 revisions, Neurology 83 (2014) 278–286.
[30] A. Ascherio, K.L. Munger, J.D. Lunemann, The initiation and prevention of multiple sclerosis, Nat. Rev. Neurol. 8 (2012) 602–612.
[31] J.C. Souberbielle, E. Cavalier, P. Delanaye, C. Massart, S. Brailly-Tabard, C. Cormier, D. Borderie, A. Benachi, P. Chanson, Serum calcitriol concentrations measured with a new direct automated assay in a large population of adult healthy subjects and in various clinical situations, Clin. Chim. Acta 451 (2015) 149–153.
[32] W.W. Hwang-Verslues, F.M. Sladek, Nuclear receptor hepatocyte nuclear factor 4alpha1 competes with oncoprotein c-Myc for control of the p21/WAF1 promoter, Mol. Endocrinol. 22 (2008) 78–90.
[33] S. Mansilla, W. Priebe, J. Portugal, Sp1-targeted inhibition of gene transcription by WP631 in transfected lymphocytes, Biochemistry 43 (2004) 7584–7592.
[34] B. Martin, A. Vaquero, W. Priebe, J. Portugal, Bisanthracycline WP631 inhibits basal and Sp1-activated transcription initiation in vitro, Nucleic Acids Res. 27 (1999) 3402–3409.
[35] M.-. Coudé, T. Braun, J. Berrou, M. Dupont, S. Bertrand, A. Masse, E. Raffoux, R. Itzykson, M. Delord, M.E. Riveiro, P. Herait, A. Baruchel, H. Dombret, C. Gardin, BET inhbitor OTX015 targets BRD2 and BRD4 and decreases c-MYC in acute leukemia cells, Oncotarget 10 (2015), 17698.
[36] A.B. Schote, J.D. Turner, J. Schiltz, C.P. Muller, Nuclear receptors in human immune cells: expression and correlations, Mol. Immunol. 44 (2007) 1436–1445.
[37] N.L. Lazarevich, D.A. Shavochkina, D.I. Fleishman, I.F. Kustova, O.V. Morozova, E. S. Chuchuev, Y.I. Patyutko, Deregulation of hepatocyte nuclear factor 4 (HNF4)as a marker of epithelial tumors progression, Exp. Oncol. 32 (2010) 167–171.
[38] Y. Zheng, J. Li, J. Ou, Regulation of hepatitis B virus core promoter by transcription factors HNF1 and HNF4 and the viral X protein, J. Virol. 78 (13) (2004) 6908.
[39] E. Bolotin, H. Liao, T.C. Ta, C. Yang, W. Hwang-Verslues, J.R. Evans, T. Jiang, F. M. Sladek, Integrated approach for the identification of human hepatocyte nuclear factor 4alpha target genes using protein binding microarrays, Hepatology 51 (2010) 642–653.
[40] I. Jelcic, F. Al Nimer, J. Wang, V. Lentsch, R. Planas, I. Jelcic, A. Madjovski, S. Ruhrmann, W. Faigle, K. Frauenknecht, C. Pinilla, R. Santos, C. Hammer, Y. Ortiz, L. Opitz, H. Gronlund, G. Rogler, O. Boyman, R. Reynolds, A. Lutterotti, M. Khademi, T. Olsson, F. Piehl, M. Sospedra, R. Martin, Memory B cells activate brain-homing, autoreactive CD4(+) T cells in multiple sclerosis, Cell 175 (2018) 85–100.e23.
[41] M. Severa, F. Rizzo, S. Srinivasan, M. Di Dario, E. Giacomini, M.C. Buscarinu, M. Cruciani, M.P. Etna, S. Sandini, R. Mechelli, A. Farina, P. Trivedi, P.J. Hertzog, M. Salvetti, C. Farina, E.M. Coccia, A cell type-specific transcriptomic approach to map B cell and monocyte type I interferon-linked pathogenic signatures in Multiple Sclerosis, J. Autoimmun. 101 (2019) 1–16.
[42] V. Rothhammer, F.J. Quintana, Environmental control of autoimmune inflammation in the central nervous system, Curr. Opin. Immunol. 43 (2016) 46–53.
[43] Y. Arnson, Y. Shoenfeld, H. Amital, Effects of tobacco smoke on immunity, inflammation and autoimmunity, J. Autoimmun. 34 (2010) J258–J265.
[44] B. Prietl, G. Treiber, T.R. Pieber, K. Amrein, Vitamin D and immune function, Nutrients 5 (2013) 2502–2521.
[45] M. Acquaviva, C. Bassani, N. Sarno, G. Dalla Costa, M. Romeo, F. Sangalli, B. Colombo, L. Moiola, V. Martinelli, G. Comi, C. Farina, Loss of circulating CD8+ CD161high T cells in primary progressive multiple sclerosis, Front. Immunol. 10 (2019) 1.
[46] J.N. Gnanaprakasam, R. Wang, MYC in regulating immunity: metabolism and beyond, Genes 8 (2017), https://doi.org/10.3390/genes8030088.
[47] J.A. Mertz, A.R. Conery, B.M. Bryant, P. Sandy, S. Balasubramanian, D.A. Mele, L. Bergeron, R.J.3. Sims, Targeting MYC dependence in cancer by inhibiting BET bromodomains, Proc. Natl. Acad. Sci. U.S.A. 108 (2011) 16669–16674.
[48] K.L. Cheung, C. Kim, M. Zhou, The functions of BET proteins in gene transcription of biology and diseases, Front. Mol. Biosci. 8 (2021), 728777.